Pergamon

Int. J. Heat Mass Transfer. Vol. 40, No. 9, pp. 2009–2017, 1997
© 1997 Elsevier Science Ltd
Printed in Great Britain. All rights reserved
0017–9310/97 $17.00+0.00

PII: S0017–9310(96)00301–8

Boiling heat transfer of a ternary refrigerant mixture inside a horizontal smooth tube

LISHENG ZHANG, EIJI HIHARA† and TAKAMOTO SAITO
Department of Mechanical Engineering, The University of Tokyo, 7-3-1 Hongo, Bunkyo-ku, Tokyo 113, Japan

and

JONG-TAEK OH
Department of Refrigeration Engineering, Yosu National Fisheries University, San 96-1, Dunduck-Dong, Yosu, Chonnam 550-250, Korea

(*Received* 5 *December* 1995 *and in final form* 12 *August* 1996)

Abstract—A theoretical model for predicting the forced convective boiling heat transfer coefficients of ternary mixtures is presented. The effect of mass diffusion near the gas–liquid interface is considered in both nucleate boiling and forced convection vaporization contributions. The predicted heat transfer coefficients are compared with experimental data, which are obtained for an HFC32 : 125 : 134a (23 : 25 : 52 wt%) mixture inside a horizontal smooth tube 6.0 mm i.d. and 4.0 m long, and in the ranges of heat flux 10–20 kW m^{-2} and of mass flux 150–400 kg m^{-2} s^{-1}. The present predictive method shows reasonable agreement with the experimental data within an accuracy of ±30%. © 1997 Elsevier Science Ltd. All rights reserved.

1. INTRODUCTION

Chlorofluorocarbons (CFCs), which have been largely used as the working fluid in air-conditioning and refrigerating machines, were phased out at the end of 1995. The production of hydrochlorofluorocarbons (HCFCs) was frozen at the same time, and will be completely phased out by the end of 2020, because of their depleting of the stratospheric ozone layer. Moreover, it is possible that the schedule of control on HCFCs will be accelerated with the development of technology. Therefore, it has become an urgent subject to develop a substitute for HCFCs.

Attention in this study was paid to the HFC32 : 125 : 134a (23 : 25 : 52 wt%) refrigerant mixture that has been suggested as the most possible candidate for HCFC22 substitutes, and its heat transfer characteristics in convective boiling were measured.

It has been known that the boiling heat transfer coefficient for a binary mixture is lower than that of an equivalent pure fluid with the same thermodynamic properties as the mixture. In a non-azeotropic binary system, the more volatile component in liquid evaporates more rapidly than the less volatile component according to the phase equilibrium. Thus, the concentration of the more volatile component in the bulk liquid is higher than that at the gas–liquid interface, while the concentration of the more volatile component at the gas–liquid interface is lower than that in the bulk vapor. Diffusions of the more volatile component from the bulk liquid to the interface and from the interface to the bulk vapor cause a reduction in heat and mass transfer performance. The more the compositions in the liquid and vapor differ, the more the heat and mass transfer coefficients are reduced. This mechanism of heat transfer degradation can be applied to multicomponent systems including ternary mixtures.

Numerous methods for predicting the nucleate pool boiling for binary mixtures have been proposed. One of the oldest noteworthy studies is on the growth of a spherical bubble in a uniformly superheated binary liquid [1, 2]. Scriven [1] arrives at a simple expression from analytical consideration of the heat and mass diffusion processes in a superheated liquid surrounding a growing vapor bubble, and the reduction rate of the bubble growth for a binary mixture, compared with that for a single-component fluid, was represented as

$$Sn = \left[1-(y-x)\left(\frac{\alpha_L}{D_L}\right)^{0.5}\left(\frac{c_{PL}}{\Delta h}\right)\left(\frac{dT}{dx}\right)\right]^{-1} \quad (1)$$

where dT/dx is the gradient of the bubble point temperature with respect to composition; x and y are the concentrations in the liquid and vapor, respectively; α_L is the liquid thermal diffusivity and D_L is the liquid diffusion coefficient. The value of Sn is always less than or equal to unity.

---

† Author to whom correspondence should be addressed.

NOMENCLATURE

d	inner diameter of tube
D	diffusion coefficient
G	mass flux
k	correction factor
M	mass flow rate
q	heat flux
T_{Gb}	bulk temperature in vapor
T_i	temperature at interface
T_{Lb}	bulk temperature in liquid
T_{sat}	refrigerant saturation temperature
T_w	wall temperature
X	quality
x_j	mass fraction of the jth component in liquid
x_{0j}	overall mass fraction of the jth component
y_j	mass fraction of the jth component in vapor.

Greek symbols

α	heat transfer coefficient or thermal diffusivity
α_b	heat transfer coefficient of nucleate pool boiling
α_f	single-phase heat transfer coefficient of liquid alone
Δh	heat of vaporization.

Subscripts

b	nucleate boiling or bulk
G	vapor
i	interface
f	forced convective vaporization
L	liquid
w	wall.

Calus and Leonidopoulus [3] have proposed the first mechanistic type of nucleate pool boiling correlation for binary mixtures equating the decrease in the heat transfer coefficient to the reduction in the bubble growth rate:

$$\frac{\alpha}{\alpha_I} = \frac{\Delta T_I}{\Delta T} = Sn \tag{2}$$

where ΔT is the wall superheat at a prescribed heat flux. ΔT_I is the ideal wall superheat based on a linear mass fraction mixing law:

$$\Delta T_I = x_1 \Delta T_1 + x_2 \Delta T_2 \tag{3}$$

where x_1, x_2 are the mass fractions, and ΔT_1, ΔT_2 are the wall superheats of each component. For binary mixtures, $x_1 + x_2 = 1$.

Stephan and Körner [4] have developed an empirical correlation for nucleate pool boiling heat transfer for binary mixtures. They noted that at a fixed heat flux the wall superheat became maximum at a similar composition as the maximum in the difference $|y-x|$ between the vapor and liquid molar concentrations. The wall superheat is correlated as a sum of the ideal wall superheat ΔT_I and the excess wall superheat ΔT_E:

$$\Delta T = \Delta T_I + \Delta T_E \tag{4}$$

$$\Delta T_E = A|y-x|\Delta T_I \tag{5}$$

$$A = A_0(0.88 + 0.12P) \tag{6}$$

where P is pressure in bars, and the value of A_0 is experimentally determined. If the value of A_0 is unknown, a value of 1.53 is recommended.

Schlünder [5] has argued the effect of heat flux and developed a boiling model using a film theory, in which the mass diffusion shell is postulated around a growing vapor bubble. Thome [6] has proposed a simple model for nucleate pool boiling of binary mixtures. Thome assumed that the compositions in the liquid and vapor were the same at the peak heat flux, and the local saturation temperature at the interface increased to the dew point temperature. Thus, the excess wall superheat was arbitrarily postulated to be equal to the difference, ΔT_{bp}, between the bubble point and dew point temperatures at the overall composition,

$$\Delta T_E = \Delta T_{bp}. \tag{7}$$

Compared with pool boiling, only a few researches on forced convective boiling for binary mixtures have been reported. Bennett and Chen [7] have proposed a correlation for binary mixtures based upon the Chen correlation [8] in which the two-phase heat transfer coefficient was expressed as the sum of a nucleate boiling contribution and a convective vaporization contribution for single-component vertical flow boiling. Bennett and Chen postulated that the nucleate boiling heat transfer coefficients could be evaluated by the drop of the effective wall superheat, resulting from the accumulation of the less volatile component near the interface. However, in their model the effect of mass transfer was considered only in the liquid.

Shock [9] theoretically analyzed the mass transfer effect in the liquid and vapor in annular flow regime. Shock concluded that the mass transfer resistance in the liquid phase was negligible in comparison with the vapor phase.

Jung *et al.* [10] have reported the experiments of horizontal flow boiling with a binary mixture of HCFC22/CFC114. Hihara *et al.* [11] obtained local boiling coefficients for the mixtures of CFC11/12,

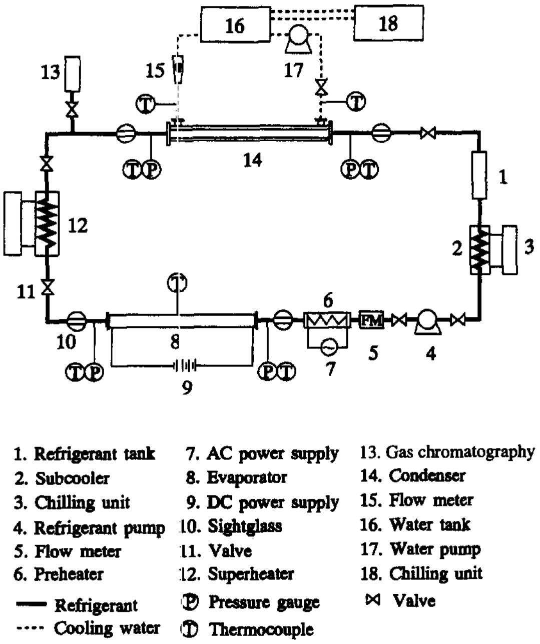

Fig. 1. Schematic diagram of the experimental apparatus.

HCFC22/CFC12 and HCFC22/CFC114 inside a horizontal smooth tube 8 mm i.d. Yoshida *et al.* [12] and Miyara *et al.* [13] have also carried out experiments for the mixtures of HCFC22/CFC114.

Hihara *et al.* [14] have presented a theoretical model for predicting the forced convective boiling heat transfer coefficients for binary systems. They modified a published heat transfer correlation for pure refrigerants by multiplying the nucleate boiling and forced convection vaporization terms by correction factors, respectively. Their model was found to fit heat transfer data for HCFC22/CFC114 to within ±30%.

So far, only a few experiments for the heat transfer of ternary refrigerant mixtures have been reported. Torikoshi *et al.* [15] carried out an experiment using tubes with extended surface for HFC32:125:134a (23:25:52 wt%), and found that the heat transfer coefficients were about 40% lower than HCFC22.

There are no published models for predicting the coefficient of convective boiling heat transfer for ternary mixtures, although it has been known that the heat transfer of ternary mixtures is much lower than the pure refrigerants. In the present study, the theoretical model [14] for binary mixtures was extended for ternary mixtures, and the predicted heat transfer coefficients were compared with experimental data obtained inside a horizontal smooth tube.

2. EXPERIMENTS

The experimental apparatus was assembled from four parts: a refrigerant loop, a cooling water system for condenser, a heat source for evaporator and a data acquisition system. A schematic of the experimental apparatus is drawn in Fig. 1. The refrigerant loop consisted of a refrigerant tank, a subcooler, a gear pump with a stepless speed change device, a mass flow meter, a preheater, an evaporator, a superheater and a condenser. Four sight glasses were installed at the evaporator inlet and outlet, and at the condenser inlet and outlet. The refrigerant was completely isolated from the lubricating oil by the use of the oil-free gear pump. The test section was the evaporator.

The evaporator was made out of four horizontal smooth stainless steel tubes with an i.d. of 6.0 mm, an o.d. of 7.0 mm and a length of 1000 mm. The total length of the evaporator was 4000 mm. The evaporator tubes were heated by applying a d.c. voltage difference along the tube. The outside wall temperatures of the tubes were measured along the tube by 24 copper–constantan thermocouples which were clamped to the tube in eight groups at axial intervals of 500 mm. At each station, the thermocouples were located at the top, side and bottom of the tube. The junctions were electrically insulated from the tube by a thin layer of Teflon tape. Measurement of refrigerant flow rate was made by a mass flow meter. The refrigerant pressures were measured by calibrated pressure gauges at the evaporator inlet and outlet. The local pressure in the test section was interpolated linearly from the measured pressures. The refrigerant temperatures were measured by chromel–alumel thermocouples at evaporator inlet, middle and outlet. The refrigerant vapor was sampled at the superheater outlet, and the composition of the vapor was analyzed with gas chromatography.

Measurement accuracy of thermocouples, refrigerant flow rate and pressure gauge was ±0.1°C, ±0.25% and ±5.3 kPa, respectively. The measurement uncertainty of the heat transfer coefficients was estimated within ±7.0%. Refrigerant mixtures used in this study were HFC32/15/134a ternary system, HFC32/134a binary system and their pure components. The experimental conditions are summarized in Table 1. Thermodynamic equilibrium properties of the mixtures were calculated from the Peng–Robinson equation of state, and transport properties were calculated using reliable predictive methods [16].

The circumferentially averaged local heat transfer coefficient is calculated by

$$\alpha = \frac{q}{T_w - T_{sat}} \tag{8}$$

where q is the heat flux, T_w is the circumferentially averaged inside wall temperature, which is calculated by solving the equation of radial heat conduction, and T_{sat} is the refrigerant saturation temperature which is calculated from the local pressure and quality.

3. PHYSICAL MODEL FOR CONVECTIVE BOILING

Forced convective boiling consists of two heat transfer mechanisms including nucleate boiling and

Table 1. Experimental conditions for convective boiling

Refrigerant	HFC32	HFC125	HFC134a	HFC32:134a	HFC32:125:134a
Composition [wt%]	100	100	100	30:70	23:25:52
Mass flux [kg m^{-2} s^{-1}]	150–400	250–450	150–400	150–400	150–400
Saturation temperature [K]	293	293	293	293	293
Heat flux [kW m^{-2}]	10–20	10–20	10–20	10–20	10–20
Quality	0–0.8	0–0.8	0–0.8	0–0.8	0–0.8

forced convective vaporization. For a low quality flow, most of the heat is transferred from the wall by nucleate boiling. For a high quality flow, nucleate boiling is suppressed due to convective effect, and most of the heat is conducted through a thin liquid film and evaporates the liquid at the gas–liquid interface. Yoshida *et al.* [17] have proposed an empirical correlation for pure refrigerants postulating the sum of a nucleate boiling contribution and a forced convective vaporization contribution:

$$\alpha = S\alpha_b + F\alpha_f \tag{9}$$

where the coefficient α_b for the nucleate boiling was evaluated using the Stephan–Abdelsalam correlation [18], and the suppression factor S due to convective effect was a function of the two-phase Reynolds number, boiling number and quality:

$$S = 1\Big/\left[1 + C\left\{\frac{G(1-X)d}{\mu_L}\frac{F^{1.25}}{10^4}\right\}^{0.5} \times \left(\frac{q\times 10^4}{G\Delta h}\right)^{-0.5} X_{tt}^{-0.5}\right]. \tag{10}$$

The forced convective vaporization contribution was the product of the single-phase heat transfer coefficient α_f for the liquid alone and a two-phase multiplier F:

$$\alpha_f = 0.023\frac{\lambda_L}{d}\left\{\frac{G(1-X)d}{\mu_L}\right\}^{0.8} Pr_L^{0.4} \tag{11}$$

$$F = 1 + 2X_{tt}^{-0.88}. \tag{12}$$

The constant C in equation (10) was experimentally determined at 0.9. In the present study, in order to fit the prediction to the present experimental data for pure refrigerants, the constant C is fixed at 0.4. The modified Yoshida correlation is compared with the experimental data for HFC32 in Fig. 2. An agreement between them is satisfactory, and similar results are obtained for HFC125 and HFC134a. For ternary mixtures the Yoshida correlation is modified by multiplying each term of nucleate boiling and forced convective vaporization by correction factors, k_b and k_f:

$$\alpha = k_b S\alpha_b + k_f F\alpha_f. \tag{13}$$

3.1. *Nucleate boiling*

In low quality regions, where nucleate boiling is the dominant mechanism for the evaporation, predictive methods for nucleate pool boiling heat transfer for multicomponent mixtures can be applied to forced convective boiling situations. In the present study, the Stephan–Körner correlation and the Thome correlation were adapted for estimating the reduction in nucleate flow boiling heat transfer.

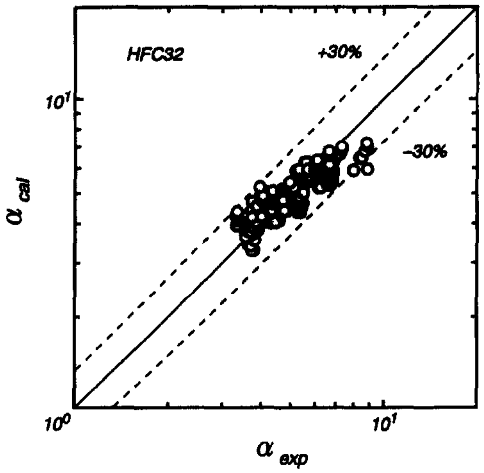

Fig. 2. Comparison of the modified Yoshida correlation with the experimental heat transfer coefficients for HFC32.

If the Stephan–Körner correlation is applied to a ternary mixture, the excess wall superheat can be extended from equation (5) as

$$\Delta T_E = A\sum_{j=1}^{3}(x_j|y_j - x_j|)\Delta T_I \tag{14}$$

$$\Delta T_I = \sum_{j=1}^{3} x_j \Delta T_j \tag{15}$$

where x_j and y_j are the mole fractions of the jth component in the liquid and vapor, respectively. The constant A_0 in equation (6) is fixed at 1.53, because nucleate pool boiling heat transfer data for HFC32/125/134a mixtures are so little that the value of A_0 cannot be determined.

The Thome correlation, applied to the estimation of nucleate flow boiling heat transfer for ternary mixtures, is in the same form as the one for binary mixtures, although the equilibrium vapor–liquid phase diagram changes from two-dimensional to three-dimensional.

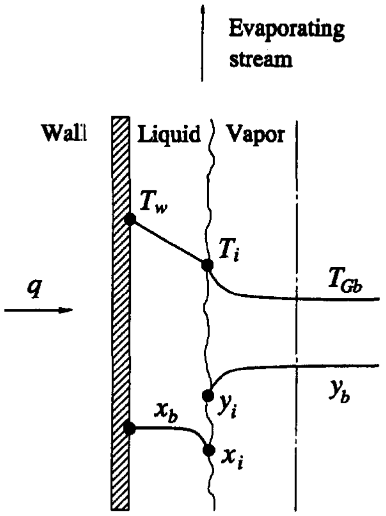

Fig. 3. Physical model of a multicomponent fluid evaporation in annular flow. Concentration profile of the most volatile component is illustrated.

The correction factor for nucleate flow boiling is expressed as

$$k_b = \frac{\Delta T_I}{\Delta T_I + \Delta T_E}. \tag{16}$$

3.2. *Forced convective vaporization*

The system model for the analysis of annular flow and an equilibrium phase diagram at a fixed pressure for a ternary mixture is illustrated in Figs. 3 and 4. As shown in Fig. 4, the interface temperature T_i is higher than the saturation temperature T_{sat} due to the mass transfer effect near the interface, and the liquid and vapor concentrations x_i, y_i on the interface satisfy the phase equilibrium. The gas–liquid interface points, x_i and y_i, are on a constant fugacity line, and the bulk points, x_b and y_b, are assumed to be on the line extended from the interface points. Three other points (x_0, x_{sat}, y_{sat}), which designate the overall composition and the imaginary equilibrium composition, are on another constant fugacity line. The following assumptions are introduced: (a) the effect of gravity is neglected and (b) the phase equilibrium prevails at the interface. Heat gained from the wall is consumed in the axial temperature rise of the liquid and vapor, and in the evaporation at the interface. Thus, a heat balance over an axial element gives

$$\pi dq = M_L C_{PL} \frac{dT_{Lb}}{dz} + M_G C_{PG} \frac{dT_{Gb}}{dz} + \pi d m_{ev} \Delta h \tag{17}$$

where m_{ev} is the evaporation rate per unit area and Δh is the heat of vaporization. The heat of vaporization is defined as the difference between vapor and liquid specific enthalpies in an equilibrium state. Axial temperature gradients in the vapor and liquid should be the same:

$$\frac{dT_{Lb}}{dz} = \frac{dT_{Gb}}{dz}. \tag{18}$$

Overall mass conservation requires

$$x_{b1} M_L + y_{b1} M_G = x_{01} M \tag{19}$$

$$x_{b2} M_L + y_{b2} M_G = x_{02} M \tag{20}$$

where x_{b1}, x_{b2}, y_{b1}, y_{b2} are the bulk mass fraction in the liquid and vapor, and x_{01}, x_{02} are the overall mass fraction of component 1 and 2, respectively.

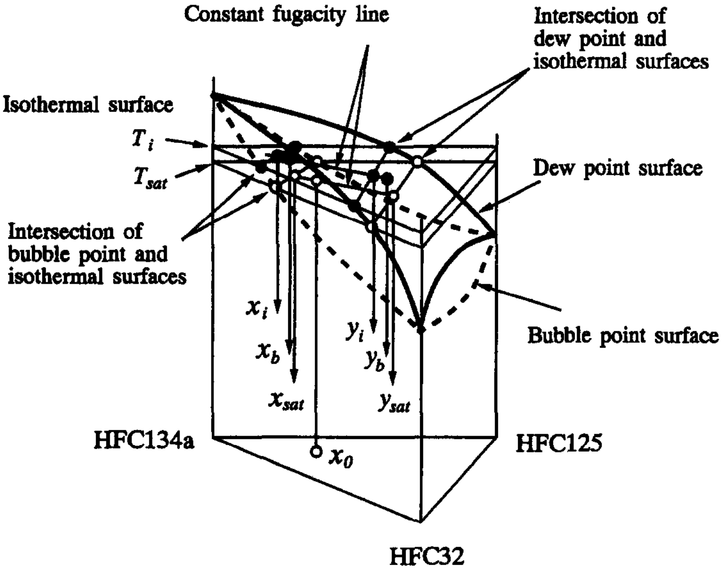

Fig. 4. A typical temperature–composition equilibrium phase diagram under a fixed pressure for a ternary mixture.

The mass transfer between the interface and the bulk vapor or liquid give

$$\alpha_{mG1}\rho_G(y_{i1}-y_{b1}) = (x_{ev1}-y_{i1})m_{ev} \quad (21)$$

$$\alpha_{mG2}\rho_G(y_{i2}-y_{b2}) = (x_{ev2}-y_{i2})m_{ev} \quad (22)$$

$$\alpha_{mL1}\rho_L(x_{b1}-x_{i1}) = (x_{ev1}-x_{i1})m_{ev} \quad (23)$$

$$\alpha_{mL2}\rho_L(x_{b2}-x_{i2}) = (x_{ev2}-x_{i2})m_{ev} \quad (24)$$

where α_{mG}, α_{mL} are the mass transfer coefficients in the vapor and liquid; x_{i1}, x_{i2}, y_{i1}, y_{i2} are the liquid and vapor phase mass fractions of component 1 and 2 on the interface; and x_{ev1}, x_{ev2} are the mass fraction in the evaporating material.

Concerning quality, the following equations are required

$$X = \frac{x_{01}-x_{sat1}}{y_{sat1}-x_{sat1}} = \frac{x_{02}-x_{sat2}}{y_{sat2}-x_{sat2}} = \frac{x_{01}-x_{b1}}{y_{b1}-x_{b1}} = \frac{x_{02}-x_{b2}}{y_{b2}-x_{b2}}. \quad (25)$$

The bulk mass fraction is determined to satisfy equation (25). The composition in the evaporating material is neither x_i nor y_i, but lies midway between them depending on the phase equilibrium of the mixture:

$$x_{ev1} = x_{i1} + \frac{y_{i1}-x_{i1}}{\dfrac{x_{01}-x_{i1}}{y_{i1}-x_{01}}\left(\dfrac{\partial T}{\partial x_{i1}}\right)\left(\dfrac{\partial y_{i1}}{\partial T}\right)+1} \quad (26)$$

$$x_{ev2} = x_{i2} + \frac{y_{i2}-x_{i2}}{\dfrac{x_{02}-x_{i2}}{y_{i2}-x_{02}}\left(\dfrac{\partial T}{\partial x_{i2}}\right)\left(\dfrac{\partial y_{i2}}{\partial T}\right)+1} \quad (27)$$

where $\partial T/\partial x_i$, $\partial T/\partial y_i$ are the slopes of the bubble point temperature line and of the dew point temperature line, respectively. The derivation of equations (26) and (27) is described in the appendix.

By analogy among momentum, heat and mass transfer, the mass transfer coefficient of component j in the vapor and liquid can be obtained:

$$\alpha_{mGj} = 0.023\frac{D_{Gj}}{d}\left(\frac{GXd}{\mu_G}\right)^{0.8} Sc_{Gj}^{0.4}F_{mG} \quad (28)$$

$$\alpha_{mLj} = 0.023\frac{D_{Lj}}{d}\left(\frac{G(1-X)d}{\mu_L}\right)^{0.8} Sc_{Lj}^{0.4}F_{mL} \quad (29)$$

where Sc_G, Sc_L are the Schmidt numbers, and F_{mG}, F_{mL} are the two-phase multipliers for mass transfer. The following two-phase multipliers [19] are adapted:

$$F_{mG} = (1+1.22X_{tt}^{0.20})^2 \quad (30)$$

$$F_{mL} = 1+21/X_{tt}+1/X_{tt}^2. \quad (31)$$

Using the interfacial temperature T_i, the correction factor for forced convective vaporization is expressed as

$$k_f = \frac{T_w-T_i}{T_w-T_{sat}}. \quad (32)$$

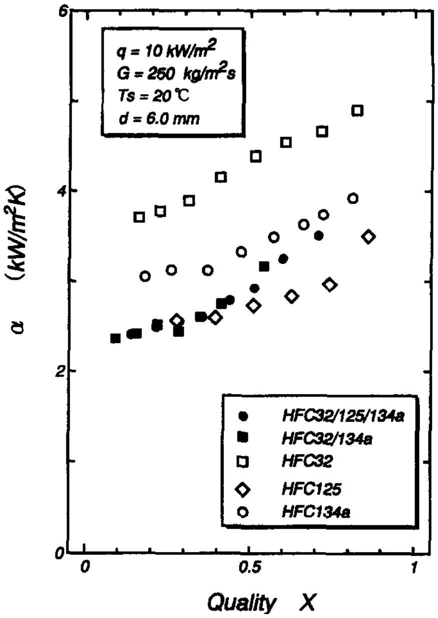

Fig. 5. Examples of the heat transfer coefficients at different qualities.

4. RESULTS AND DISCUSSIONS

4.1. *Examples of experimental results*

Figure 5 shows examples of experimental results of forced convective boiling for HFC32, HFC125, HFC134a, HFC32/134a and HFC32/125/134a. For all refrigerants, the heat transfer coefficients increase with quality. Comparing all refrigerants, HFC32 has the highest performance because of its excellent thermophysical properties. HFC32/125/134a shows about 20% lower than HFC134a in lower quality regions, but is similar to HFC134a in higher quality regions.

Figure 6 shows dependence of mass flux on the boiling heat transfer coefficient for HFC32, HFC125, HFC134a and HFC32/125/134a. For all refrigerants, the heat transfer coefficients increase with mass flux. As shown in Figs. 5 and 6 for the ternary mixture, for low qualities or for low mass fluxes a significant reduction in the heat transfer coefficient is observed. Because in these conditions the contribution of nucleate boiling is predominant, it means that the effect of mass transfer is significant in nucleate boiling.

Figure 7 shows a comparison of the experimental heat transfer coefficients for HFC32/125/134a with the modified Yoshida correlation. Because the mass transfer effects are not considered in the modified Yoshida correlation, about 30% degradation in heat transfer is observed, especially in low quality regions.

4.2. *Mass transfer effect in liquid phase*

In order to calculate the effect of mass transfer resistance in both phases, the forced convection vaporization in equations (17)–(31) is simplified for binary mixtures. The concentration gradients due to mass transfer effects cause a rise of the interface tempera-

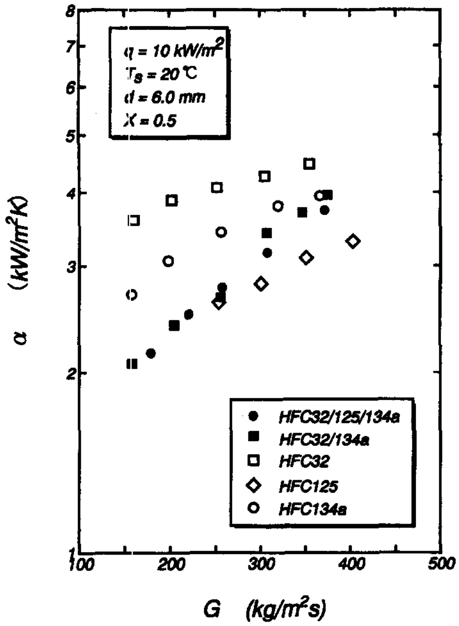

Fig. 6. Examples of the heat transfer coefficients at different mass fluxes for $X = 0.5$.

ture, and so the amount of mass transfer effects can be estimated using the rise of the interface temperature. Four models of mass transfer resistance are calculated; in model 1 the resistances in the liquid and vapor phases are both considered; in model 2 the resistance is considered only in the vapor phase; model 3 includes only the liquid phase resistance; and model 4 does not consider any resistance. Comparing four models for an HFC32/134a binary mixture in Fig. 8, interface temperatures of models 3 and 4 coincide with each other, therefore it can be concluded that the mass transfer resistance in the liquid phase is negligible, and dominant resistance to mass transfer exists in the vapor phase. These results coincide with Shock's analysis [9].

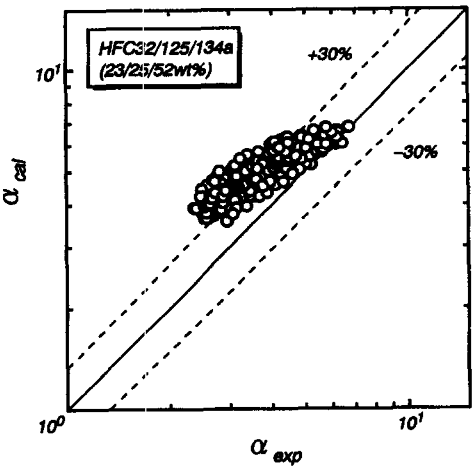

Fig. 7. Comparison of the modified Yoshida correlation with the experimental heat transfer coefficients for HFC32/125/134a mixture.

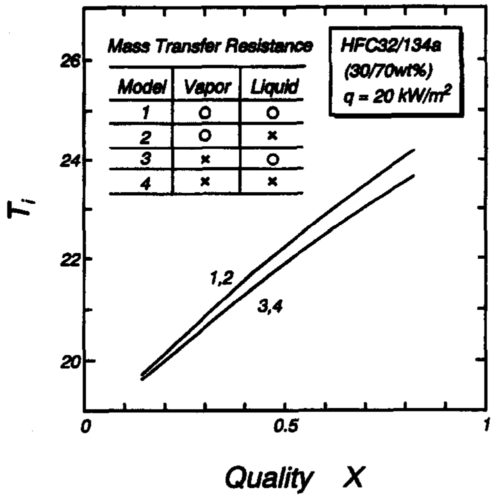

Fig. 8. Effect of the resistance to mass transfer in the liquid and vapor phases on the interface temperature for HFC32/134a mixture.

The mass transfer effects in both phases should also be examined for the ternary mixture, but it is impossible to calculate the mass transfer coefficient in the liquid, because no predictive method for diffusion coefficient for ternary liquid mixtures has been established. Therefore, applying the results in the binary mixture correspondingly to the ternary mixture, the mass transfer effect in the liquid phase is neglected in the present model. From this assumption, $x_{b1} = x_{i1}$, $x_{b2} = x_{i2}$, and equations (23) and (24) are omitted from the theory.

4.3. *Comparison of the present model with the data*

Reduction factors of the heat transfer coefficients of nucleate boiling and forced convective vaporization for HFC32/125/134a are compared in Fig. 9. For nucleate boiling, the Thome correlation is much lower

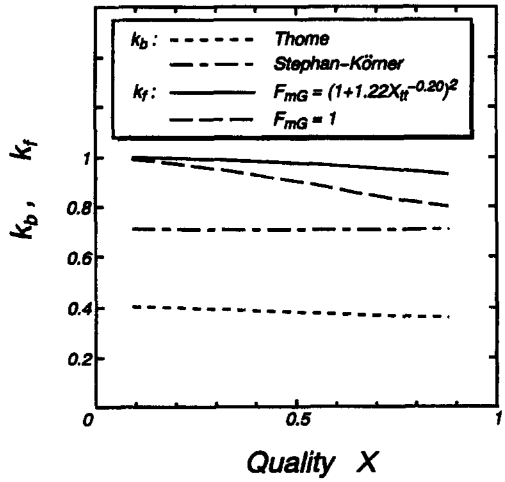

Fig. 9. Correction factors of heat transfer coefficients in the nucleate boiling and in the forced convective vaporization for HFC32/125/134a mixture, $G = 310$ kg m^{-2} s^{-1}, and $q = 20$ kW m^{-2}.

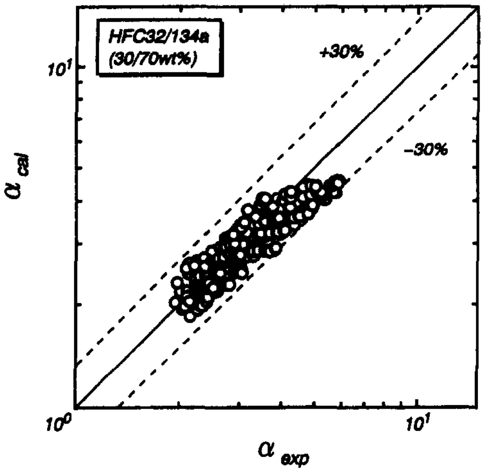

Fig. 10. Comparison of the present model based on the Thome correlation with the experimental heat transfer coefficients for HFC32/134a mixture.

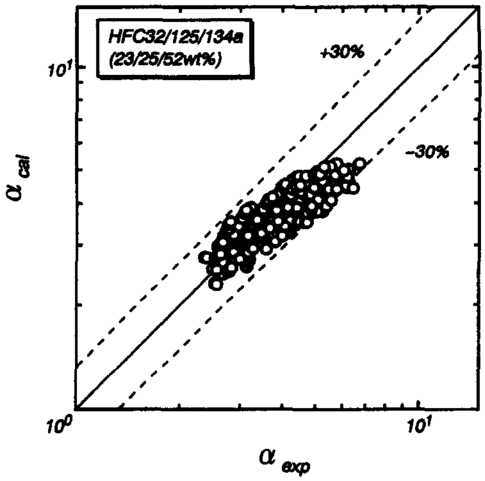

Fig. 12. Comparison of the present model, based on the Thome correlation and assumed $F_{mG} = 1$, with the experimental heat transfer coefficients for HFC32/125/134a mixture.

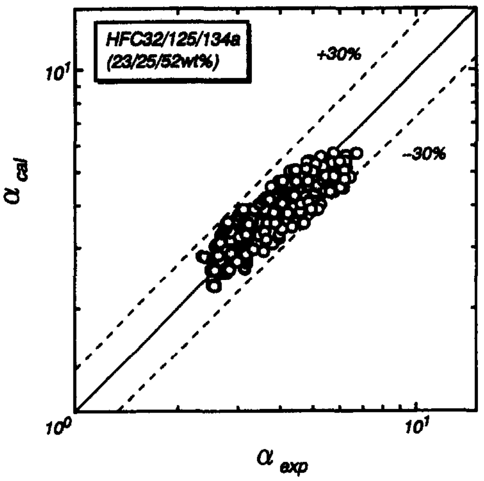

Fig. 11. Comparison of the present model based on the Thome correlation with the experimental heat transfer coefficients for HFC32/125/134a mixture.

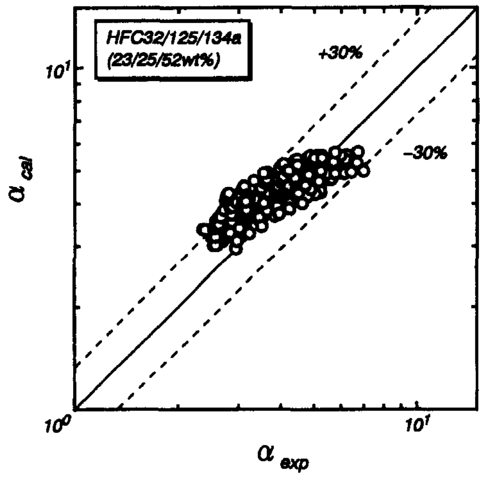

Fig. 13. Comparison of the present model based on the Stephan–Körner correlation with the experimental heat transfer coefficients for HFC32/125/134a mixture.

than the Stephan–Körner correlation. The difference between the Thome and Stephan–Körner correlations is important in low quality or low mass flux conditions where S is relatively large, but in high quality or high mass flux conditions, where S is small, the difference between these correlations does not influence the heat transfer coefficient α. For the forced convective vaporization, the effect of a two-phase multiplier for mass transfer is also shown in Fig. 9. The reduction rate of the forced convective vaporization heat transfer is less than 5%, while if the two-phase multiplier is neglected, namely, $F_{mG} = 1$, the reduction rate becomes up to 20%.

Figures 10 and 11 show comparisons of the experimental heat transfer coefficients with the present model based on the Thome correlation for HFC32/134a and HFC32/125/134a, respectively. The predictions satisfactorily fit the experimental results to within ±30%. If the two-phase multiplier for mass transfer is assumed to be unity, the predicted heat transfer coefficients at high qualities become lower than the experimental coefficients (see Fig. 12). This means that an enhancement of the mass transfer in the vapor by the interfacial movements should be considered. Figure 13 demonstrates a comparison of the present model based on the Stephan–Körner correlation with the experimental heat transfer coefficients. This model overpredicts heat transfer by approximately 15%.

Comparing Figs. 10–13, it can be concluded that for the nucleate boiling contribution the Thome correlation is appropriate, and for the forced convection vaporization contribution the present model provides a reasonable prediction.

5. CONCLUSIONS

The forced convective boiling heat transfer coefficients of a ternary mixture HFC32/125/134a and a binary mixture HFC32/134a were measured inside a horizontal smooth tube. Because both mixtures were non-azeotropic, on average the heat transfer coefficients were 30% lower than HFC134a due to the mass transfer resistance near the gas–liquid interface. The heat transfer coefficients were significantly reduced especially in low quality and low mass flux regions.

A method for predicting the heat transfer coefficients of ternary refrigerant mixtures was presented. Considering the mass transfer effect, the nucleate boiling contribution was modified by the Thome correlation, and the forced convection vaporization contribution was modified by the annular flow model. Basically, these modifications were similar to the treatment for binary mixtures. Model predictions were in satisfactory agreement with the experimental heat transfer coefficients. This result indicates that there is no essential difference in the mechanisms of boiling heat transfer of binary and ternary mixtures.

Acknowledgements—Support of this work by the Ministry of Education of Japan under Grant No. 06452182 and Mitsubishi Electric Co. is gratefully acknowledged.

REFERENCES

1. L. E. Scriven, On the dynamics of phase growth, *Chem. Engng Sci.* **10**, 1–13 (1959).
2. S. J. D. Van Stralen, Bubble growth rates in boiling binary mixtures, *Br. Chem. Engng* **12**, 238–250 (1967).
3. W. F. Calus and D. J. Leonidopoulos, Pool boiling—binary liquid mixtures, *Int. J. Heat Mass Transfer* **17**, 249–256 (1974).
4. K. Stephan and M. Körner, Calculation of heat transfer in evaporating binary mixtures, *Chemie Ingr. Tech.* **41**, 409–417 (1969).
5. E. U. Schlünder, Heat transfer in nucleate boiling of mixtures, *Int. Chem. Engng* **23**, 589–599 (1983).
6. J. R. Thome, Prediction of binary mixture boiling heat transfer coefficients using only phase equilibrium data, *Int. J. Heat Mass Transfer* **26**, 965–974 (1983).
7. D. L. Bennett and J. C. Chen, Forced convective boiling in vertical tubes for saturated pure components and binary mixtures, *A.I.Ch.E. Jl* **26**, 454–461 (1980).
8. J. C. Chen, Correlation for boiling heat transfer to saturated fluids in convective flow, *I & EC Proc. Des. Dev.* **5**, 322–329 (1966).
9. R. A. W. Shock, Evaporation of binary mixtures in upward annular flow, *Int. J. Multiphase Flow* **2**, 411–433 (1976).
10. D. S. Jung, M. McLinden, R. Radermacher and D. Didion, Horizontal flow boiling heat transfer experiments with a mixture of R22/R114, *Int. J. Heat Mass Transfer* **32**, 131–145 (1989).
11. E. Hihara and T. Saito, Forced convective boiling experiments of binary mixtures, *JSME Int. J.* Ser. II **32**, 98–106 (1989).
12. S. Yoshida, H. Mori, T. Matsunaga and K. Oishi, Heat transfer to non-azeotropic mixtures of refrigerants flowing in a horizontal evaporator tube, *Trans. JSME B* **56,** 198–203 (1990).
13. A. Miyara, H. Takamatsu, S. Koyama, K. Yonemoto and T. Fujii, Forced convective boiling of nonazeotropic refrigerant mixtures of R22 and R114 inside a horizontal tube, *Trans. JSME B* **54,** 2523–2528 (1988).
14. E. Hihara and T. Saito, Forced convective boiling heat transfer of binary mixtures in a horizontal tube, *Proceedings of the Ninth International Heat Transfer Conference*, Vol. 2, pp. 123–128, Hemisphere, Jerusalem (1990).
15. K. Torikoshi, T. Ebisu, K. Toda and H. Onishi, Heat transfer of ternary non-azeotropic mixtures inside a grooved horizontal tube, *Proceedings of the 28th Japanese Joint Conference on Air-Conditioning and Refrigeration*, pp. 145–148, Tokyo (1994).
16. R. C. Reid, J. M. Prausnitz and B. E. Poling, *The Properties of Gases and Liquids*. McGraw-Hill, Maidenhead, U.K. (1987).
17. S. Yoshida, H. Mori, H. Hong and T. Matsunaga, Prediction of heat transfer coefficient for refrigerants flowing in horizontal evaporator tubes, *Trans. JAR* **11,** 67–78 (1994).
18. K. Stephan and M. Abdelsalam, Heat transfer correlations for natural convection boiling, *Int. J. Heat Mass Transfer* **23,** 73–87 (1980).
19. T. Ueda and M. Inoue, Heat transfer during annular flow condensation of steam inside tubes, *Trans. JSME B* **43,** 233–240 (1977).

APPENDIX

Derivation of composition in evaporating material

A ternary mixture in an equilibrium state evaporates under a constant pressure. Assuming that the saturation temperature increases from T to $T+\Delta T$, the concentrations in the liquid and vapor change from x_j, y_j into $x'_j = x_j+(\partial x_j/\partial T)\Delta T$, $y'_j = y_j+(\partial y_j/\partial T)\Delta T$ ($j = 1,2$), where $(\partial T/\partial x_j)$ and $(\partial T/\partial y_j)$ are the slopes of bubble point temperature line and of dew point temperature line according to the concentration of the jth component, respectively. Expressing the overall composition as x_{0j}, the quality also changes from $X = (x_{0j}-x_j)/(y_j-x_j)$ into $X' = (x_{0j}-x'_j)/(y'_j-x'_j)$. The mass conservations of the jth component in the liquid and vapor are

$$x_j(1-X)-x'_j(1-X') = x_{\mathrm{ev}j}(X'-X) \quad (j = 1,2)$$

$$y_jX-y'_jX' = x_{\mathrm{ev}j}(X-X') \quad (j = 1,2).$$

Elimination of X' and simple manipulation lead to

$$x_{\mathrm{ev}j} = x_j+\frac{y_j-x_j}{\dfrac{x_{0j}-x_j}{y_j-x_{0j}}\left(\dfrac{\partial T}{\partial x_j}\right)\left(\dfrac{\partial y_j}{\partial T}\right)+1} \quad (j = 1,2).$$